中国光学 Chinese Optics 核心期刊

偏振激光雷达增益比定标方法对比研究

童奕澄 童学东 张凯 肖达 戎宇航 周雨迪 刘崇 刘东

Polarization lidar gain ratio calibration method: a comparison

TONG Yi-cheng, TONG Xue-dong, ZHANG Kai, XIAO Da, RONG Yu-hang, ZHOU Yu-di, LIU Chong, LIU Dong

引用本文:
童奕澄, 童学东, 张凯, 肖达, 戎宇航, 周雨迪, 刘崇, 刘东. 偏振激光雷达增益比定标方法对比研究[J]. 中国光学, 2021, 14(3): 685–703. doi: 10.37188/CO.2020–0136
TONG Yi-cheng, TONG Xue-dong, ZHANG Kai, XIAO Da, RONG Yu-hang, ZHOU Yu-di, LIU Chong, LIU Dong. Polarization lidar gain ratio calibration method: a comparison[J]. *Chinese Optics*, 2021, 14(3): 685-703. doi: 10.37188/CO.2020-0136

在线阅读 View online: https://doi.org/10.37188/CO.2020–0136

文章编号 2095-1531(2021)03-0685-19

Polarization lidar gain ratio calibration method: a comparison

TONG Yi-cheng[1], TONG Xue-dong[2], ZHANG Kai[1], XIAO Da[1], RONG Yu-hang[1], ZHOU Yu-di[1,3], LIU Chong[1], LIU Dong[1*]

(1. *State Key Laboratory of Modern Optical Instrumentation*, *College of Optical Science and Engineering*, *Zhejiang University*, *Hangzhou* 310027, *China*;
2. *NingBo Iron & Steel Co.*, *Ltd.*, *Ningbo* 315807, *China*;
3. *Ningbo Research Institute*, *Zhejiang University*, *Ningbo* 315100, *China*)
* *Corresponding author*, *E-mail*: *liudongopt@zju.edu.cn*

Abstract: Gain ratio calibration error is one of the most significant factors affecting the accuracy of a polarization lidar depolarization ratio. This paper analyzes the basic principles of various existing gain ratio calibration methods and compares the advantages and disadvantages of the +45° method, ±45° method, Δ45° method, rotation fitting method and pseudo-depolarizer method in practice though experiments. Results show that: the Δ45° method, ±45° method and rotation fitting method are relatively accurate when the misalignment angle is small, but the operation of the ±45° method and rotation fitting method are more complicated. The +45° method still has a large calibration error without a misalignment angle. The pseudo-depolarizer method is the easiest to operate, but it is restricted by a non-ideal pseudo-depolarizer. Through comparison of theory and experiment, this paper provides a suggestion for the best choice of gain ratio calibration method. It is recommended that the ±45° method be used for calibration with a half-wave plate, and the pseudo-depolarizer method be used for calibration with a high-precision depolarizer.

Key words: polarization lidar; gain ratio; calibration; depolarization ratio

偏振激光雷达增益比定标方法对比研究

童奕澄[1], 童学东[2], 张 凯[1], 肖 达[1], 戎宇航[1], 周雨迪[1,3], 刘 崇[1], 刘 东[1*]

(1. 浙江大学 光电科学与工程学院 现代光学仪器国家重点实验室, 浙江 杭州 310027;
2. 宁波钢铁有限公司 浙江 宁波 315807;
3. 浙江大学 宁波研究院 浙江 宁波 315100)

摘要: 增益比定标误差是影响偏振激光雷达退偏比精度的主要因素之一, 观测前必须进行准确的增益比定标。本文分析

收稿日期: 2020-08-10; **修订日期:** 2020-09-11

基金项目: 国家重点研发计划(No. 2016YFC1400900); 国家自然科学基金(No. 41775023); 浙江省自然科学基金杰出青年项目 (No. LR19D050001)

Supported by National Key Research and Development Program of China (No. 2016YFC1400900); National Natural Science Foundation of China (No. 41775023); Excellent Young Scientist Program of Zhejiang Provincial Natural Science Foundation of China (No. LR19D050001)

了现存多种增益比定标方法的基本原理,并通过实验对比了+45°法、±45°法、Δ45°法、旋转拟合法与退偏器法等增益比定标方法的定标准确性与优缺点。实验结果表明:Δ45°法、±45°法与旋转拟合法在对准偏失角较小的情况下定标相对准确,但±45°法与旋转拟合法操作较为繁琐。+45°法在无对准偏失角的情况下定标误差仍较大。退偏器法操作最简便,但会受到非理想退偏器的制约。通过理论分析与实验对比,本文给出了增益比定标方法的最佳选择,即在一般情况下采用Δ45°法定标,在有高精度退偏器的情况下采用退偏器法定标。

关 键 词: 偏振激光雷达;增益比;定标;退偏比

中图分类号: TP958.98 **文献标志码:** A **doi:** 10.37188/CO.2020-0136

1 Introduction

Polarization lidar is one of the earliest members of lidar family. Since its birth in 1971, polarization lidar has become a research tool widely used in atmospheric cloud and aerosol detection[1]. The depolarization ratio obtained by polarization lidar inversion can be used to distinguish spherical and non-spherical particles, so it is often applied to the identification of aerosol type and the identification of thermodynamic phase state of clouds[2]. Moreover, the depolarization ratio can also be used to identify the tropospheric boundary layer and to distinguish polar stratospheric clouds from other types of clouds in terms of morphology[3-5]. At the same time, the depolarization ratio can be used to study the long-distance transmission characteristics of dust[6]. It can be seen that the high-precision detection of depolarization ratio is of great significance to atmospheric science research. However, how to improve the detection accuracy of depolarization ratio has always been the research focus of polarization lidar[7].

The main causes for depolarization ratio error include: the calibration error of polarization lidar gain ratio, the error caused by the impurity of laser ray polarization, the alignment angle error between laser polarization vector and Polarization Beam Splitter (PBS) incidence plane, as well as the polarization crosstalk error caused when the reflectance and transmittance of PBS cannot reach 100%. In order to simplify the description, the above four errors are referred to as gain ratio calibration error, linear polarization error, alignment angle error and polarization crosstalk error respectively. Among them, gain ratio calibration error is particularly important and has a decisive effect on the accuracy of depolarization ratio[8]. The gain ratio calibration error varies with the gain ratio calibration method. For nearly half a century, more and more researchers have proposed new gain ratio calibration methods. However, there is still a lack of effective guidance and suggestions on the selection of gain ratio calibration method in the actual use of polarization lidar.

This paper analyzes the basic principles of various existing gain ratio calibration methods and compares the accuracy and advantages and disadvantages of +45° method, +45° method, Δ45° method, rotation fitting method and pseudo-depolarizer method at different misalignment angles through experiments. Through the comparison of theory and experiment, this paper provides a suggestion for the best choice of gain ratio calibration method.

2 Basic principles and structure

The typical polarization lidar is a two-channel lidar[1]. According to the definition of depolarization ratio δ[9], we can obtain

$$\delta=\frac{\beta_{\perp}}{\beta_{\parallel}}=\frac{P_{\perp}}{P_{\parallel}}\quad , \tag{1}$$

where β represents atmospheric backscattering coefficient, P represents the echo signal power, and the subscripts $\perp$ and $\parallel$ respectively represent the vertical and parallel components of the above parameters.

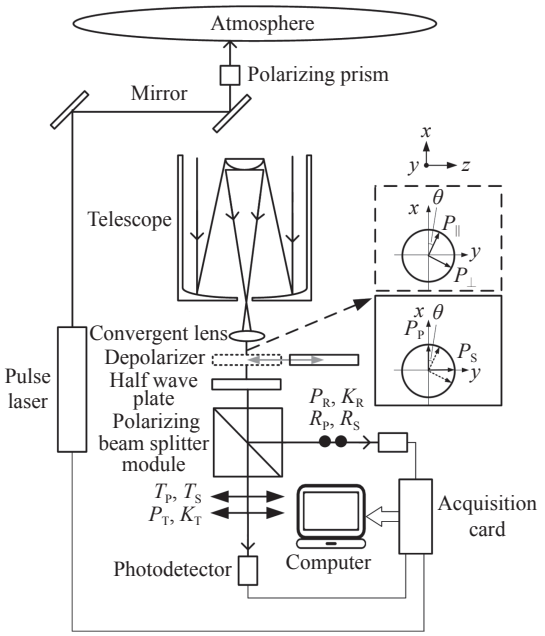

Fig. 1　Basic principle and structure diagram of polarization lidar system

图 1　偏振激光雷达系统基本原理与结构图

As shown in Fig. 1. the vertical component $P_{\perp}$ and parallel component $P_{\parallel}$ of echo signal can be decomposed into the following components after the coordinate rotation transformation relative to the incident plane of PBS:

$$\begin{cases} P_{S'}(\theta) = P_{\perp}\cos^2(\theta) + P_{\parallel}\sin^2(\theta) \\ P_{P'}(\theta) = P_{\perp}\sin^2(\theta) + P_{\parallel}\cos^2(\theta) \end{cases}, \tag{2}$$

where the subscripts S' and P' respectively represent the directions perpendicular to and parallel to the incident plane of PBS, and θ represents the angle between the laser polarization vector and the incident plane of PBS (here referred to as misalignment angle).

Because there is polarization crosstalk in the actual PBS, the parameters R_P, R_S, T_P and T_S respectively represent the reflectance and transmittance ratios of P and S light in PBS (the above four parameters are generally known, and are labeled by PBS manufacturer). After the light passes through the PBS, the detected power P_R and P_T in the reflection channel and transmission channel can be expressed as

$$\begin{cases} P_R(\theta) = [P_{P'}(\theta)R_P + P_{S'}(\theta)R_S]K_R \\ P_T(\theta) = [P_{P'}(\theta)T_P + P_{S'}(\theta)T_S]K_T \end{cases}, \tag{3}$$

where K_R and K_T respectively represent the gain coefficients of reflection channel and transmission channel, $G=K_R/K_T$. According to the Eq. (3), the actually measured depolarization ratio $\delta^*(\theta)$ can be obtained:

$$\delta^*(\theta) = \frac{P_R(\theta)}{P_T(\theta)} = \frac{[1+\delta\tan^2(\theta)]R_P + [\tan^2(\theta)+\delta]R_S}{[1+\delta\tan^2(\theta)]T_P + [\tan^2(\theta)+\delta]T_S}\cdot G \quad . \tag{4}$$

It can be seen from the equations (1) ~ (4) that the gain ratio G must be calibrated before the calculation of the depolarization ratio, and that the gain ratio calibration error will affect the calculation result of the depolarization ratio[10]. Next, we will introduce several typical gain-ratio calibration methods.

3　Gain ratio calibration methods

3.1　Method of clean atmospheric molecule

The method of clean atmospheric molecule is a method to calibrate the gain ratio by comparing the actual depolarization ratio of clean atmosphere detected by the system and the theoretical depolarization ratio of clean atmosphere, assuming that only atmospheric molecules (no aerosols and clouds) exist in the high air. The calculation formula of depolarization ratio in the method of clean atmospheric molecule is

$$\delta_{mol} = \frac{\beta_{\perp}^{m}}{\beta_{\parallel}^{m}} \quad , \tag{5}$$

where $\beta_{\perp}^{m}$ and $\beta_{\parallel}^{m}$ respectively represent the vertical and horizontal components of the backscattering coefficient of atmospheric molecules. In the experiment, a relatively clean atmospheric area at the altitude r_c was selected, where only atmospheric molecules could exist. It should be noted that the influence of misalignment angle and polarization crosstalk is generally not considered in the method of clean atmospheric molecule (i.e., θ=0°, R_S=T_P=1, R_P=T_S= 0). Therefore, the gain ratio G can be calculated by Eq. (4):

$$G = \frac{\delta^*}{\delta_{mol}} \quad , \tag{6}$$

where δ^* and δ_{mol} respectively represent the atmospheric molecular depolarization ratio actually measured at the altitude r_c and the theoretical atmospheric molecular depolarization ratio. δ_{mol} can be calculated according to the theory of atmospheric scattering[11], but it is not fixed. Atmospheric molecular scattering is mainly composed of Rayleigh scattering and vibration Raman scattering (with a negligible intensity). Rayleigh scattering is mainly composed of pure rotational Raman line and central Cabannes line[12]. In the Rayleigh scattering spectrum, Cabannes lines constitute the central peak of Doppler broadening, while pure rotational Raman lines are distributed on both sides of Cabannes lines to constitute the sidebands[13]. The depolarization effect caused by pure rotational Raman lines is much greater than that caused by Cabannes lines. For a lidar system, the value range of δ_{mol} is between 0.003 63~0.014 3 when the filters with different bandwidths (BWs) are used[10]. If the filter bandwidth in the lidar system is narrow (BW<0.3 nm @532 nm), δ_{mol} will be the lower limit, namely δ_{mol}=0.003 63. Conversely, if the filter bandwidth is wide (BW=15 nm@532 nm), δ_{mol} will be the upper limit, namely δ_{mol}=0.014 3.

Due to convenient operation and no need to add other devices to the light path of the system, the method of clean atmospheric molecule was widely used in the 1980s and 1990s. However, its shortcoming is also very obvious. Because clean atmosphere rarely exists, the calibration result obtained from a calibration area with aerosols or clouds present will have a large error. Moreover, when the filter bandwidth ranges from 1 nm to 15 nm, the proportion of pure rotational Raman lines in the scattered atmospheric molecules cannot be accurately evaluated. This may lead to the inaccurate calculation of the theoretical depolarization ratio of clean atmosphere, resulting in a calibration error. In addition, it should be noted that the method of clean atmospheric molecule is generally applicable to the lidar with a laser wavelength of less than 550 nm. For the lidar with a detection wavelength of more than 800 nm, this calibration method is likely to cause a large calibration error because the Rayleigh scattering intensity is weak[13]. Therefore, this method is rarely used at present.

3.2 +45° method

+45° method is a method of placing a Half-Wave Plate (HWP) in the receiving optical path (generally in front of PBS) and rotating it in one direction (clockwise/counterclockwise) to realize the gain ratio calibration. In particular, this method assumes that the properties of HWP are ideal and that the atmospheric state does not change during calibration. In addition to the above two basic assumptions, two more assumptions should be added to the +45° method, that is, neither a misalignment angle nor polarization crosstalk will exist[14].

As shown in Fig. 2 (Color online), the HWP is placed in the upstream optical path of PBS. In this case, the laser polarization vector is considered to be parallel to the incident plane of PBS, as shown in Fig. 2(a).

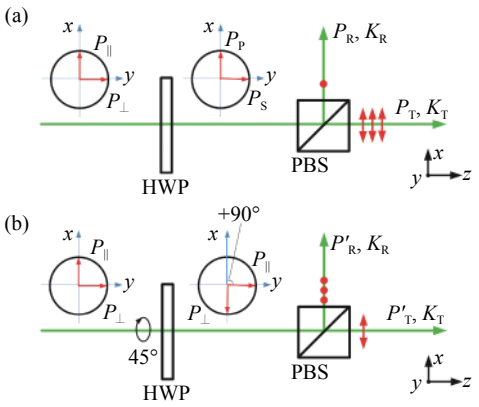

Fig. 2 Schematic diagram of +45° method. (a) Before HWP rotation. (b) After HWP rotation by +45°

图 2 +45°法原理图。(a) 半波片旋转之前; (b) 半波片旋转+45°之后

Since the impact of misalignment angle and polarization crosstalk is not considered, the Eq. (3) can be simplified as

$$\begin{cases} P_R(0°) = P_S(0°)K_R \\ P_T(0°) = P_P(0°)K_T \end{cases}. \quad (7)$$

Then, the HWP is rotated clockwise around the optical axis (similar to the counterclockwise case), so the angle between the laser polarization vector and the incident plane of PBS is +90°, as shown in

Fig. 2(b). In the Eq. (7), $P_T(0°)$ becomes $P'_T(90°)$. The specific formula is not repeated here. In this case, the gain ratio G can be expressed as

$$G = \frac{P_R(0°)}{P'_T(90°)} \quad . \tag{8}$$

The advantage of this method is easy operation. Its disadvantage is that the alignment angle error and polarization crosstalk error can be easily introduced as the effects of misalignment angle and polarization crosstalk are ignored.

3.3　±45° method

±45° method is a method of placing a HWP in the receiving optical path and rotating it twice (by +22.5° and −22.5° respectively relative to the initial position) to realize the gain ratio calibration. This method was proposed by Freudenthaler *et al*. from the University of Munich, Germany[15]. Based on the +45° method, the ±45° method has considered the effects of both misalignment angle and polarization crosstalk. As shown in Fig. 3 (Color online).

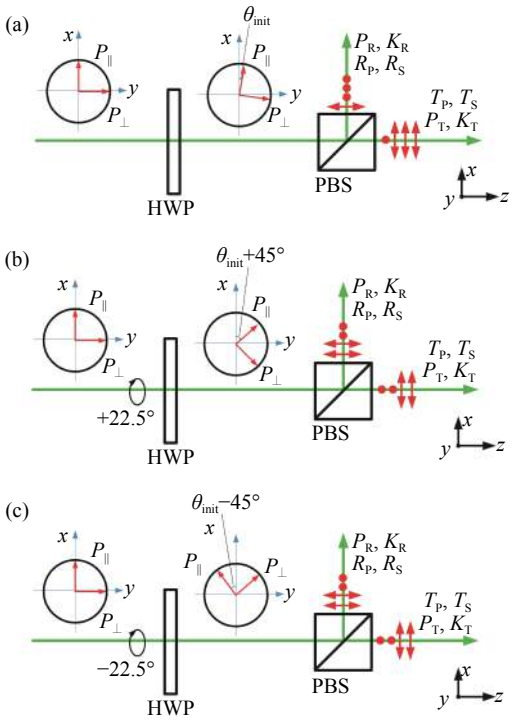

Fig. 3　Schematic diagram of ±45° method. (a) Before HWP rotation. (b) After HWP rotation by +22.5°. (c) After HWP rotation by −22.5°

图 3　±45°法原理图。(a) 半波片旋转之前; (b) 半波片旋转+22.5°之后; (c) 半波片旋转−22.5°之后

In Fig. 3, a HWP is placed in the upstream optical path of PBS. It is assumed that there is an initial misalignment angle θ_{init} between the laser polarization vector and the incident surface of PBS, and that θ_h is the quantitative misalignment angle introduced artificially.

After the HWP rotation, the following equation can be derived from Eq. (4):

$$\delta^*(\theta_{init}+\theta_h) = \frac{P_R(\theta_{init}+\theta_h)}{P_T(\theta_{init}+\theta_h)} = \frac{[1+\delta\tan^2(\theta_{init}+\theta_h)]R_P + [\tan^2(\theta_{init}+\theta_h)+\delta]R_S}{[1+\delta\tan^2(\theta_{init}+\theta_h)]T_P + [\tan^2(\theta_{init}+\theta_h)+\delta]T_S}\cdot G, \tag{9}$$

In order to reduce the influence of initial misalignment angle θ_{init}, the HWP is rotated twice continuously in the ±45° method. At first, the HWP is rotated by +22.5° clockwise around the optical axis relative to its initial position. Then, the HWP is rotated by −45° counterclockwise around the optical axis based on the first rotation, or by −22.5° counterclockwise around the optical axis relative to its initial position. In the two rotations, the angles between the laser polarization vector and the incident surface of PBS are +45° and −45° respectively. At this time, the gain ratio G can be expressed as

$$G = \frac{T_P+T_S}{R_P+R_S}\cdot\sqrt{\delta^*(\theta_{init}+45)\,\delta^*(\theta_{init}-45)} \quad . \tag{10}$$

It can be seen from Eq. (10) that in the ±45° method, the polarization crosstalk error of PBS is considered, but the influence of alignment angle error cannot be completely eliminated. It is proved by facts that the error source has little to do with the Signal-to-Noise Ratio (SNR) in the ±45° method[16]. If θ_{init} = 1°, the relative error of G can be controlled within 5%[15]. With the advantages of simple operation and high accuracy, the ±45° method has been used in MULIS (Multichannel Lidar System), POLIS (Portable Lidar System) and other high-precision polarization lidar systems for gain ratio calibration[16]. Its shortcoming is that the alignment angle error cannot be eliminated.

3.4　Δ45° method

Δ45° method is a method of placing a HWP in

the receiving optical path and rotating it by 45° in one direction (clockwise/counterclockwise) to realize the gain ratio calibration. This method has the same operation as +45° method, but different calculation approach. In addition, it doesn't need initial 0° search. This method was proposed by Luo Jing *et al*. from Zhejiang University[17], as shown in Fig. 4 (Color online).

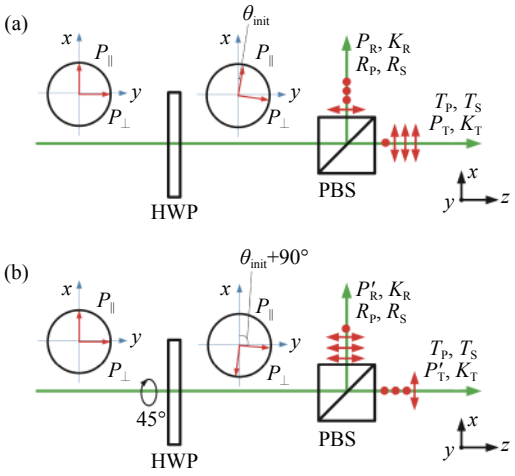

Fig. 4 Schematic diagram of Δ45° method. (a) Before HWP rotation. (b) After HWP rotation by 45°

图 4 Δ45°法原理图。(a) 半波片旋转之前; (b) 半波片旋转 45°之后

In Fig. 4, a HWP is placed in the upstream optical path of PBS. It is assumed that there is an initial misalignment angle between the laser polarization vector and the incident surface of PBS.

Before the HWP rotation, the following equation can be derived from Eq. (4):

$$\begin{cases} P_R(\theta_{init}) = \left\{\left[P_{S'}\sin^2(\theta_{init}) + P_{P'}\cos^2(\theta_{init})\right]R_P + \right. \\ \quad \left.\left[P_{S'}\cos^2(\theta_{init}) + P_{P'}\sin^2(\theta_{init})\right]R_S\right\}K_R \\ P_T(\theta_{init}) = \left\{\left[P_{S'}\sin^2(\theta_{init}) + P_{P'}\cos^2(\theta_{init})\right]T_P + \right. \\ \quad \left.\left[P_{S'}\cos^2(\theta_{init}) + P_{P'}\sin^2(\theta_{init})\right]T_S\right\}K_T \end{cases}. \quad (11)$$

Then, the HWP is rotated around the optical axis, as shown in Fig. 4(b). After rotation, the terms $P_R(\theta_{init})$ and $P_T(\theta_{init})$ in Eq. (11) turn into $P'_R(\theta_{init}+90°)$ and $P'_T(\theta_{init}+90°)$. The specific formula is not repeated here. In this case, the gain ratio can be expressed as

$$G = \frac{P_R(\theta_{init}) + P'_R(\theta_{init}+90°)}{P_T(\theta_{init}) + P'_T(\theta_{init}+90°)} \cdot \frac{T_P + T_S}{R_P + R_S}, \quad (12)$$

where $P_T(\theta_{init})$, $P_R(\theta_{init})$, $P'_T(\theta_{init}+90°)$ and $P'_R(\theta_{init}+90°)$ can be considered as known quantities. It can be seen from Eq. (12) that Δ45° method not only eliminates the alignment angle error, but also reduces the polarization crosstalk error. Moreover, the initial direction of laser polarization vector can be arbitrary, which reduces the need to adjust the orientation of HWP fast axis before rotating the HWP. Δ45° method can not only improve the calibration speed, but also ensure the calibration accuracy. Its disadvantage is that the influence of atmospheric state change cannot be eliminated.

3.5 Rotation fitting method

Rotation fitting method is a method of placing a HWP in the receiving optical path and rotating it for several times to realize the gain ratio calibration through the nonlinear least square fitting and the inversion of gain ratio, depolarization ratio and initial misalignment angle θ_{init}[18]. This method was proposed by Alvarez *et al*. from NASA.

As shown in Fig. 5 (Color online), a HWP is placed in the upstream optical path of PBS. It is assumed that there is an initial misalignment angle θ_{init} between the laser polarization vector and the incident surface of PBS.

If the HWP is rotated artificially by $\theta_{h,j}/2$ relative to its initial optical axis, a series of misalignment angles $\theta_{h,j}$ can be introduced artificially and quantitatively. From Eq. (9), the following equation can be derived:

$$\delta^*(\theta_{init}+\theta_{h,j}) = \frac{P_R(\theta_{init}+\theta_{h,j})}{P_T(\theta_{init}+\theta_{h,j})} = \frac{[1+\delta\tan^2(\theta_{init}+\theta_{h,j})]R_P + [\tan^2(\theta_{init}+\theta_{h,j})+\delta]R_S}{[1+\delta\tan^2(\theta_{init}+\theta_{h,j})]T_P + [\tan^2(\theta_{init}+\theta_{h,j})+\delta]T_S} \cdot G, \quad (13)$$

where j represents the j-th rotation of the HWP. In the Eq. (13), as $\delta^*(\theta_{init}+\theta_{h,j})$, $\theta_{h,j}$, R_P, R_S, T_P and T_S can be considered as known quantities, only three quantities, namely gain ratio G, initial misalignment angle θ_{init} and theoretical depolarization ratio δ, are unknown. In this case, the three unknowns cannot be

solved by a single equation. However, multiple equations can be obtained by rotating the HWP for many times. Then the nonlinear least square method can be used to solve the equation set so as to solve the three unknowns. It should be noted that at least three equations need to be obtained in this method, namely $j \geqslant 3$.

The advantage of this method is that the three unknowns, namely gain ratio, depolarization ratio and initial misalignment angle, can be inverted simultaneously through one calibration, and no a priori value is required. However, due to time-consuming calibration and complicated operation, this method is only suitable for a relatively stable atmospheric environment.

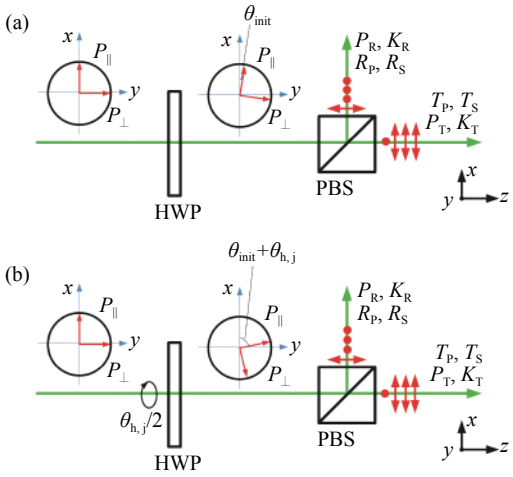

Fig. 5　Schematic diagram of rotation fitting method. (a) Before HWP rotation. (b) After HWP rotation by $\theta_{h,j}$

图 5　旋转拟合法原理图。(a) 半波片旋转之前; (b) 半波片旋转$\theta_{h,j}$角之后

3.6　Pseudo-depolarizer method

The pseudo-depolarizer method is a method that adds an optical element to the optical path to convert the echo signal received by the system into unpolarized light so as to realize the gain ratio calibration. The gain ratio is calibrated by using the ratio of signal intensities of two detection channels. From Eq. (4), the gain ratio G can be obtained:

$$G=\frac{P_{\mathrm{R}}}{P_{\mathrm{T}}} \quad . \qquad (14)$$

A typical example is found in the CALIOP, where the non-depolarizing signal generated by a depolarizer is used for gain ratio calibration[19]. The specific operation procedure is as follows. A movable depolarizer is placed in the upstream optical path of PBS during the system calibration, and is removed after the calibration completion, as shown in Fig. 6. In the CALIOP, this method is used to calibrate the gain ratio of the system on orbit at night and then the method of clean atmospheric molecule is used to verify the calibration result[20].

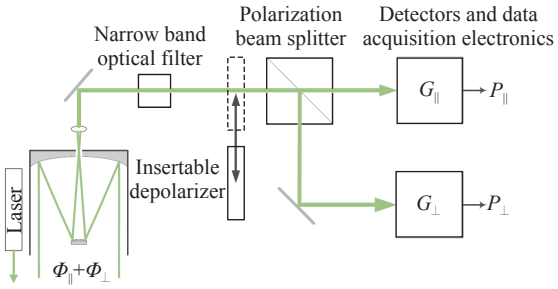

Fig. 6　Schematic diagram for CALIOP gain ratio calibration

图 6　CALIOP 增益比定标原理图

The advantage of this method is that it can be operated easily and calibrated in real time, so as to eliminate the influence of atmospheric state change. Its disadvantage is that other errors will be introduced easily due to the difficulty for a commercial depolarizer to produce completely depolarized light.

4　Experimental results and analysis

The polarization lidar used in the experiment is a typical dual-channel lidar, whose structure is shown in Fig. 1 (where the same device is only marked once). The pseudo-depolarizer between the convergent lens and the HWP is only used in the pseudo-depolarizer method. To reduce linear polarization error, a polarizing prism was added to the emergent light path in the experiment system, so that the extinction ratio of the outgoing laser reached $2\times10^5:1$. To reduce the polarization crosstalk error, a PBS was glued with a polarizing film to achieve $T_{\mathrm{P}}:T_{\mathrm{S}}(R_{\mathrm{S}}:R_{\mathrm{P}})>30\,000:1$. Therefore, the effect of alignment error on gain ratio is

discussed instead of the effect of linear polarization error and polarization crosstalk error. The specific parameters of the system are shown in Table 1.

Tab. 1 Main parameters for polarization lidar system
表 1 偏振激光雷达系统主要参数

Main parameters	Value
Laser center wavelength	532 nm
Laser energy	5 mJ
Repetition frequency	10 Hz
Pulse width	8 ns
Diameter of telescope primary mirror	210 mm
Field of view of telescope	1 mrad
Focal length of telescope	2000 mm
Filter bandwidth	3 nm

Due to the large calibration error of clean atmospheric molecules, the experiment in this paper mainly compares the influence of five methods, namely, +45° method, ±45° method, Δ45° method, rotation fitting method and pseudo-depolarizer method, on the gain ratio calibration at different misalignment angles (alignment angle errors).

To ensure a high signal-to-noise ratio, the experiment was carried out at night. Meanwhile, in order to reduce the impact caused by atmospheric changes, the detection in horizontal direction (pitch angle: 0°) was adopted. After the optical axis calibration of the system was completed, an electric rotating motor (accuracy: 0.005°) was used to adjust the half-wave plate to the position where the laser polarization vector was parallel to the incident surface of PBS (when 200 signals on average were passed and the maximum power of transmission channel was detected visually). At this point, the HWP angle was the initial 0°. It should be noted that, for the convenience of description, the initial misalignment angle θ_{init} is not included in the actual total misalignment angle when the misalignment angle θ_h is introduced artificially and quantitatively to the following section. However, each actual misalignment angle contains the initial misalignment angle θ_{init} (an unknown quantity). Then, with θ_h=0° (the actual misalignment angle is θ_{init}+0°) as the zero point, an electric rotating motor is used to rotate the HWP. In the actual operation, the alignment angle usually does not exceed 15°[21-22]. However, to ensure the experiment integrity, the misalignment angle under discussion is expanded to 45° in this paper.

In the +45° method, ±45° method, Δ45° method and rotation fitting method, the HWP was rotated with a step size of 2.5° within the θ_h range of −45°~67.5° to obtain a total of 46 sets of original echo signals. By processing the above data, a step size of 5° and a θ_h range of −45° ~ +45° (that is, the difference between the two angles in each group of data before and after the HWP rotation are 45°) were selected in the four methods. After calculation, a total of 19 groups of gain ratio data were obtained.

Before starting the experiment, a pseudo-depolarizer was added to the optical path of the system, as shown in Fig. 1. Since the pseudo-depolarizer was not ideal, the HWP was rotated with a step size of 10° within the θ_h range of −80° ~ +100° to obtain a total of 19 sets of original echo signals in order to observe the change of pseudo-depolarizer in at least one cycle. By processing the above data, a total of 19 groups of gain ratio data were obtained after calculation.

The calibration results of the above five methods are given in Table 2 (θ_h=0°).

Tab. 2 Calibration results of five methods at θ_h=0°
表 2 θ_h=0°时 5 种方法的定标结果

	Calibration method				
	+45°	±45°	△45°	Rotation fitting	Pseudo-depolarizer
Calibration result	1.2185±0.1379	1.2679±0.1518	1.2676±0.1524	1.2716±0.0250	1.1977±0.1483

As can be seen from Table 2, when there is no misalignment angle (θ_h=0°), the calibration results of ±45° method, Δ45° method and rotation fitting method are close to each other and can be considered closest to the true value. Therefore, the average value of the gain ratios measured by the above three methods at θ_h=0° is defined as the true value. The curves of the relative errors of the five calibration methods changing with the misalignment angle are shown in Fig. 7 (the calculation processes of rotation fitting method and pseudo-deflector method are described in detail in the Sections 4.2 and 4.3).

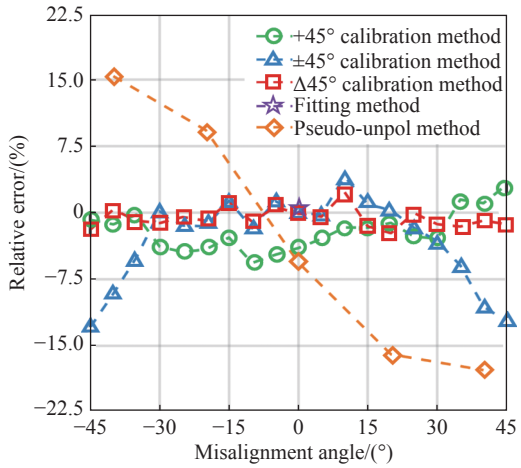

Fig. 7　Relative errors changing with the misalignment angle for the five calibration methods

图 7　5 种定标方法相对误差随对准偏失角的变化曲线

4.1　+45°, ±45° and Δ45° methods

As shown in Fig. 7, when $|\theta_h|$<15°, the calibration results of ±45° method and Δ45° method are similar with a small relative error. However, even if the misalignment angle is 0°, the calibration result of +45° method is still greatly different from those of the above two methods, with a relative error up to 4%. When $|\theta_h|$>15°, the calibration results of +45° method and Δ45° method will remain almost stable. However, with the increase of misalignment angle, the calibration result of ±45° method will become more unstable and its relative error will increase sharply even up to 12.93%. The main reason for such error distribution is that the ±45° method calculates the geometric average of the two measurements before and after rotation, while the Δ45° method calculates the arithmetic average of the two measurements before and after rotation based on the +45° method. The reasons for the above phenomena of +45° method will be explained below through specific theoretical analysis.

The relative error between the two methods was analyzed[23-24]. The powers detected in the reflection channel and transmission channel before and after the HWP rotation in the two methods are denoted as P_R^a, P_R^b and P_T^a, P_T^b. Then

$$(\delta_1)^2=\left(\frac{\Delta G_{\Delta 45^\circ}}{G_{\Delta 45^\circ}}\right)^2=\frac{(\Delta P_R^a)^2+(\Delta P_R^b)^2}{(P_R^a+P_R^b)^2}+\frac{(\Delta P_T^a)^2+(\Delta P_T^b)^2}{(P_T^a+P_T^b)^2}\quad,\qquad(15)$$

$$(\delta_2)^2=\left(\frac{\Delta G_{+45^\circ}}{G_{+45^\circ}}\right)^2=\frac{1}{4}\left(\frac{\Delta P_R^a}{P_R^a}\right)^2+\frac{1}{4}\left(\frac{\Delta P_R^b}{P_R^b}\right)^2+\frac{1}{4}\left(\frac{\Delta P_T^a}{P_T^a}\right)^2+\frac{1}{4}\left(\frac{\Delta P_T^b}{P_T^b}\right)^2\quad,\qquad(16)$$

where δ_1 and δ_2 represent the relative errors of the calibration results of Δ45° method and ±45° method, and ΔP_S^n (S is R or T and n is a or b) represents the uncertainty (standard deviation) in each measured value. The photon counting signal in lidar can be considered to be subject to Poisson distribution[25-26], so the statistical error is equal to the root mean square of the mean value of the signal, i.e. $\Delta I=\sqrt{I}$. Therefore, the equations (15) and (16) can be further deduced as follows

$$(\delta_1)^2=\frac{1}{P_R^a+P_R^b}+\frac{1}{P_T^a+P_T^b}\quad,\qquad(17)$$

$$(\delta_2)^2=\frac{1}{4P_R^a}+\frac{1}{4P_R^b}+\frac{1}{4P_T^a}+\frac{1}{4P_T^b}\quad.\qquad(18)$$

It can be found that $(\delta_1)^2\leqslant(\delta_2)^2$, that is, the uncertainty of Δ45° method is less than or equal to that of ±45° method. According to the experimental results, when the misalignment angle is large, the oscillation amplitude of gain ratio profile of ±45° calibration method is indeed greater than that of Δ45° method. This also explains why the error of ±45° method in Fig. 7 is much greater than that of Δ45° method when the alignment angle is large.

4.2 Rotation fitting method

Considering that the error of misalignment angle was not greater than 15° in the actual process, 13 sets of data satisfying $|\theta_h| \leqslant 15°$ (that is, $\theta_{h,j}$ = 0°, ±2.5°, ±5° ⋯ ±15°) were selected for fitting. The calculation results of rotation fitting are shown in Fig. 8 (Color online). According to Eq. (13), solving the three unknowns (gain ratio G, initial misalignment angle θ_{init} and theoretical depolarization ratio δ) in the equations is a nonlinear least square problem. Before solving G, θ_{init} and δ, their initial values need to be predicted. Their optimum initial predicted values are shown in Fig. 8.

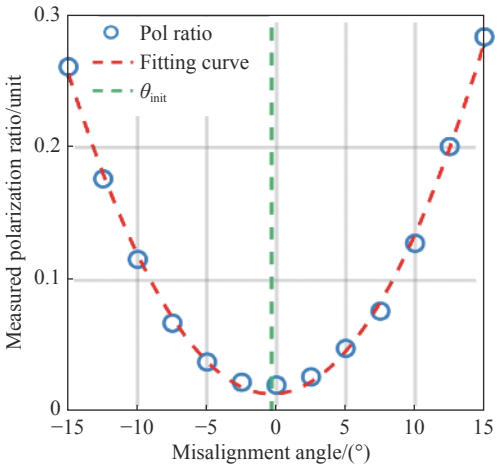

Fig. 8 Curve of the actually measured depolarization ratio changing with the misalignment angle, where the blue circle represents the $\delta^*(\theta)$ values measured at different θ angles, and the red and green dotted lines represent the fitting curve and θ_{init}, respectively

图 8 实际测量退偏比随对准偏失角的变化曲线图。其中蓝色圆圈代表在不同θ情况下测量的$\delta^*(\theta)$, 红色虚线代表拟合曲线, 绿色虚线代表θ_{init}

It can be found that the relationship between $\delta^*(\theta_{init}+\theta_{h,j})$ and $\theta_{h,j}$ (blue circle) can be approximately represented by a quadratic polynomial[27]. Therefore, the following quadratic polynomial is constructed with the artificially and quantitatively introduced misalignment angle $\theta_{h,j}$ as an independent variable and the actually measured depolarization ratio $\delta^*(\theta_{init}+\theta_{h,j})$ as a dependent variable:

$$\delta^*(\theta_{init}+\theta_{h,j})^*=A_0+A_1\times\theta_{h,j}+A_2\times\theta_{h,j}^{\ 2} \quad , \qquad (19)$$

where A_0, A_1 and A_2 are quadratic polynomial coefficients. The fitting result is shown as the red dotted line in Fig. 8. The minimum value of the quadratic polynomial represents the initial misalignment angle θ_{init}, whose result is calculated to be $\theta_{init} = -A_1/(2\times A_2) = -0.35°$. This value can be used as the optimum initial predicted value of θ_{init}. Then, θ_{init} = −0.35° is substituted into Eq. (13) and the equation set is solved with nonlinear least square method to obtain the gain ratio, namely G=1.271 6.

4.3 Pseudo-depolarizer method

The calculation result of pseudo-depolarizer method is shown in Fig. 9 (Color online), in which the blue circles represent the gain ratios calculated at different angles of the HWP. It can be observed that the distribution of blue circles is in line with the cosine curve distribution law. Therefore, the following cosine function polynomial is constructed with the HWP rotation angle φ (θ_h=2φ) as an independent variable and the gain ratio G as a dependent variable:

$$G=B_0\cos(B_1\times\varphi+B_2)+B_3 \quad , \qquad (20)$$

where B_0, B_1, B_2 and B_3 all represent the coefficients of the cosine function polynomial. The fitting result is shown as the red dotted line in Fig. 9.

Theoretically, if the echo signal is completely unpolarized light, its state will remain unchanged, irrespective of how the HWP angle is changed. In other words, the rotation of HWP will not affect the value of gain ratio. The result of gain ratio calibration should be represented by a line parallel to the x-axis, rather than by a cosine curve as shown in Fig. 9. The reason for this problem is that the existing commercial depolarizer cannot completely transform the polarized light into unpolarized light, so that the echo signal still contains part of the polarized light after passing through the depolarizer. When using laser as the light source to test the depolarizing effect of a depolarizer, Luo Jing et al. from Zhejiang University found that the test result was similar to the cosine distribution in Fig. 9[28]. This indicates that the result of gain ratio calibration will still be affected by this portion of polar-

ized light even if the misalignment angle is 0°.

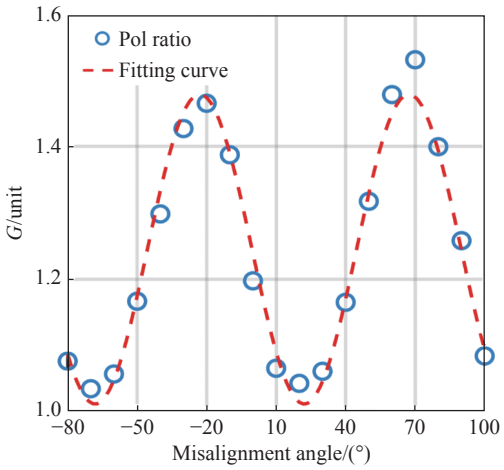

Fig. 9　Gain ratio calibration result of pseudo-depolarizer method. The blue circles represent the gain ratios measured at different misalignment angles, and the red dotted line represents the cosine polynomial fitting curve

图 9　退偏器法增益比定标结果。蓝色圆圈代表半波片在不同角度下测量的增益比，红色虚线代表余弦函数多项式拟合曲线

It should be noted that among the measurement data obtained by pseudo-depolarizer method, only 5 sets of data satisfy $\theta_h = -45° \sim +45°$. Therefore, only 5 points are marked in Fig. 7 according to this method. At $\theta_h = 0°$, the relative error of pseudo-depolarizer method is 5.6%. This indicates that the result of gain ratio calibration will still be affected by this portion of polarized light even if the misalignment angle is 0°.

4.4　Discussion

Through the analysis of experimental results, we know that the calibration results of ±45° method, Δ45° method and rotation fitting method are the most accurate. This is consistent with the above theoretical analysis result. However, the error of ±45° method will increase with the misalignment angle. The rotation fitting method is only suitable for a relatively stable atmospheric environment due to time-consuming calibration and complicated operation. In comparison, Δ45° method has obvious advantages: easier operation, robust calibration results not affected by misalignment angle, and no need to search for the initial 0° angle. However, Δ45° method cannot eliminate the influence of atmospheric state changes. In contrast, the pseudo-depolarizer method is not only easy to operate, but also capable of eliminating the influence of atmospheric state changes and free from the problem that multiple HWP rotations will increase the accumulated angle error. But so far, the commercial depolarizer still cannot produce completely depolarized light, which will introduce a new error that is difficult to evaluate. In conclusion, we suggest the use of Δ45° method for calibration as a general rule and the use of pseudo-depolarizer method for calibration when a high-precision depolarizer is available.

5　Conclusion

The calibration accuracy of gain ratio has a great influence on the detection accuracy of polarization lidar. This paper compares a variety of the existing gain-ratio calibration methods theoretically and experimentally for the first time, and provides some suggestions on the selection of gain-ratio calibration methods.

As far as the operability is concerned, the pseudo-depolarizer method only needs a depolarizer inserted into the system to realize the calibration, and can eliminate the influence of atmospheric state changes. The other four methods require at least two rotations of the HWP in relatively complicated operation and cannot eliminate the influence of atmospheric state changes. In terms of calibration accuracy, this experiment mainly compared the influence of +45° method, ±45° method, Δ45° method, rotation fitting method and pseudo-depolarizer method (excluding the method of clean atmospheric molecule due to its large calibration error) on the gain ratio calibration at different misalignment angles. The experimental results show that the calibration accuracy of ±45° method, Δ45° method and rotation fitting method is relatively high, but the operation of ±45° method and rotation fitting method is quite complex. The error of ±45° method is big when the misalignment angle is large. In the Δ45° method, the result of gain ratio calibration is not af-

fected by the misalignment angle, and there is no need to search for the initial 0° angle. Compared with the first three methods, +45° method has a larger error when the misalignment angle is 0°. The pseudo-depolarizer method is greatly affected by the use of non-ideal depolarizer. If an ideal depolarizer is available, this method will be an ideal gain-ratio calibration method. By comparing different gain-ratio calibration methods theoretically and experimentally, this paper gives the best choice of gain ratio calibration method, suggesting the use of Δ45° method for calibration as a general rule and the use of pseudo-depolarizer method for calibration when a high-precision depolarizer is available.

——中文对照版——

1 引 言

偏振激光雷达是激光雷达家族中最早的成员之一，自 1971 年诞生以来，其已广泛应用于大气云及气溶胶探测[1]。偏振激光雷达反演得到的退偏比可用于区分球形粒子和非球形粒子，故其常被应用于气溶胶的类型识别及云的热力学相态识别[2]。不仅如此，退偏比也可用于识别对流层的边界层以及从形态学上区分极地平流层云与其它种类云[3-5]。同时，退偏比还可以用于研究沙尘的长距离传输特性[6]。可见，实现退偏比的高精度探测对大气科学研究具有重要的意义。然而，如何提高退偏比的探测精度，一直以来都是偏振激光雷达的研究重点[7]。

退偏比误差产生的主要原因包括：偏振激光雷达增益比的定标误差、发射激光线偏振度不纯而引起的误差、激光偏振矢量与偏振分光棱镜（Polarization Beam Splitter, PBS）入射面的对准角误差以及 PBS 反射、透过率无法达到 100% 而引起的偏振串扰误差。为了简化描述，本文分别简称上述 4 种误差为增益比定标误差、线偏振度误差、对准角误差与偏振串扰误差，其中增益比定标误差大小对退偏比的精度起着决定作用[8]。不同增益比定标方法所产生的增益比定标误差也不同。近半个世纪，不断有研究人员提出新的增益比定标方法，然而到目前为止，偏振激光雷达在实际使用过程中对增益比定标方法的选择依旧缺少有效的指导与建议。

本文介绍了现存多种增益比定标方法的基本原理，并通过实验对比分析了+45°法、±45°法、Δ45°法、旋转拟合法与退偏器法在不同对准偏失角情况下增益比定标的准确性以及各自的优缺点。通过理论与实验的对比，本文给出了增益比定标方法的最佳选择。

2 基本原理与结构

目前常见的偏振激光雷达为双通道的激光雷达[1]，根据退偏比δ[9] 的定义，可得

$$\delta=\frac{\beta_{\perp}}{\beta_{\parallel}}=\frac{P_{\perp}}{P_{\parallel}}\quad , \tag{1}$$

式中，β代表大气后向散射系数，P代表回波信号功率，下标$\perp$与$\parallel$分别代表上述各参量的垂直与平行分量。如图 1 所示，回波信号垂直分量$P_{\perp}$与平行分量$P_{\parallel}$相对于 PBS 入射面在经坐标旋转变换后可分解为

$$\begin{cases}P_{S'}(\theta)=P_{\perp}\cos^2(\theta)+P_{\parallel}\sin^2(\theta)\\ P_{P'}(\theta)=P_{\perp}\sin^2(\theta)+P_{\parallel}\cos^2(\theta)\end{cases}. \tag{2}$$

式中，下标S'与P'分别代表与 PBS 入射面垂直方向及平行方向，θ代表激光偏振矢量与 PBS 入射面存在的夹角（此处称为对准偏失角）。

由于实际的 PBS 存在偏振串扰，因此，定义R_{P}、R_{S}、T_{P}与T_{S}分别代表 PBS 对 P 光与 S 光的反射率与透过率（以上 4 个参数一般由 PBS 生产商标称出，属于已知量）。经过 PBS 后反射通道与透射通道被探测到的功率P_{R}、P_{T}分别可表示为

$$\begin{cases}P_{\mathrm{R}}(\theta)=[P_{P'}(\theta)R_{\mathrm{P}}+P_{S'}(\theta)R_{\mathrm{S}}]K_{\mathrm{R}}\\ P_{\mathrm{T}}(\theta)=[P_{P'}(\theta)T_{\mathrm{P}}+P_{S'}(\theta)T_{\mathrm{S}}]K_{\mathrm{T}}\end{cases}, \tag{3}$$

式中K_{R}与K_{T}分别代表反射通道与透射通道的增益系数。其中$G=K_{\mathrm{R}}/K_{\mathrm{T}}$，根据式（3）可得实际测量退偏比$\delta^*(\theta)$

$$\delta^{*}(\theta)=\frac{P_{\mathrm{R}}(\theta)}{P_{\mathrm{T}}(\theta)}=\frac{[1+\delta\tan^{2}(\theta)]R_{\mathrm{P}}+[\tan^{2}(\theta)+\delta]R_{\mathrm{S}}}{[1+\delta\tan^{2}(\theta)]T_{\mathrm{P}}+[\tan^{2}(\theta)+\delta]T_{\mathrm{S}}}\cdot G\quad .\tag{4}$$

由式(1)~式(4)可知, 在计算退偏比之前必须完成增益比G的定标, 而增益比定标的误差会对退偏比的计算结果造成影响[10]。接下来本文将介绍几种常用的增益比定标方法。

3　增益比定标方法

3.1　洁净大气分子法

洁净大气分子法是假定高空中只存在大气分子(无气溶胶与云), 通过对比系统探测洁净大气实际退偏比与洁净大气理论退偏比以完成增益比定标的方法。洁净大气分子法退偏比的计算公式为

$$\delta_{\mathrm{mol}}=\frac{\beta_{\perp}^{\mathrm{m}}}{\beta_{\parallel}^{\mathrm{m}}}\quad ,\tag{5}$$

式中, $\beta_{\perp}^{\mathrm{m}}$与$\beta_{\parallel}^{\mathrm{m}}$分别代表大气分子后向散射系数的垂直分量与水平分量。实验中, 选择较为洁净且高度为r_{c}的大气区域, 此区域可认为只有大气分子存在。需要注意的是, 洁净大气分子法一般来说并不考虑对准偏失角与偏振串扰的影响(即θ=0°、R_{S}=T_{P}=1、R_{P}=T_{S}=0), 所以由式(4)可求解增益比G

$$G=\frac{\delta^{*}}{\delta_{\mathrm{mol}}}\quad ,\tag{6}$$

式中, δ^{*}与δ_{mol}在此处分别代表高度为r_{c}处实际测量大气分子退偏比与理论大气分子的退偏比。δ_{mol}可以根据大气散射理论[11]计算得到, 但是该理论值并不固定。由于大气分子散射主要由瑞利散射与振动拉曼散射(该散射强度很小, 可忽略不计)组成, 其中瑞利散射主要由纯转动拉曼线与中心Cabannes线组成[12]。在瑞利散射光谱结构中, Cabannes线属于多普勒展宽的中央峰, 纯转动拉曼线分布在Cabannes线的两侧, 属于边带[13], 纯转动拉曼线造成的退偏效果比Cabannes线大得多。对于激光雷达系统说, 使用不同带宽(Bandwidth, BW)的滤光片, δ_{mol}取值范围在0.00363~0.01423之间[10]。如果激光雷达系统中滤光片的带宽较窄(BW<0.3 nm@532 nm), δ_{mol}=0.00363。反之, 如果滤光片的带宽较宽(BW=15 nm@532 nm), 则δ_{mol}=0.01423。

洁净大气分子法由于操作比较方便, 且不需要在系统光路中添加其它器件, 所以该定标方法在上世纪末使用较为广泛, 但其缺点也很明显, 因为真正洁净的大气很少存在, 若选取的定标区域存在气溶胶或云, 定标结果将会产生较大误差, 而且当滤光片带宽在1~15 nm时, 由于无法准确评估纯转动拉曼线在大气分子散射中所占的比例, 可能导致洁净大气理论退偏比计算不准确, 从而造成定标误差。另外, 需要注意的是, 洁净大气分子法一般适用于激光波长小于550 nm的激光雷达。对于探测波长大于800 nm的激光雷达, 由于瑞利散射强度较小, 使用该定标方法易造成较大的定标误差[13]。因此, 该方法目前很少被采用。

3.2　+45°法

+45°法是一种将半波片(Half-Wave Plate, HWP)置于接收光路中(一般置于PBS前), 通过单方向(顺/逆时针均可)旋转半波片以完成增益比定标的方法。需要特别说明的是, 该方法假设半波片的性质理想, 且定标时大气状态不发生改变。对于+45°法, 除了以上两个基本假设外, 还需要增加另外两个假设, 即不存在对准偏失角, 也不存在偏振串扰[14]。

如图2(彩图见期刊电子版)所示, 首先将半波片放置于PBS上游光路中, 此时认为激光偏振矢量与PBS入射面平行, 如图2(a)所示。

此时由于不考虑对准偏失角和偏振串扰的影响, 式(3)可简化为

$$\begin{cases}P_{\mathrm{R}}(0°)=P_{\mathrm{S}}(0°)K_{\mathrm{R}}\\ P_{\mathrm{T}}(0°)=P_{\mathrm{P}}(0°)K_{\mathrm{T}}\end{cases}\quad .\tag{7}$$

然后将半波片绕光轴顺时针旋转(逆时针类似), 使得激光偏振矢量与PBS入射面成+90°, 如图2(b)所示, 式(7)中的$P_{\mathrm{T}}(0°)$变为$P_{\mathrm{T}}'(90°)$, 具体公式不再赘述, 此时增益比G可表示为

$$G=\frac{P_{\mathrm{R}}(0°)}{P_{\mathrm{T}}'(90°)}\quad .\tag{8}$$

该方法的优点是操作较简便, 缺点为忽略了对准偏失角和偏振串扰的影响, 易引入对准角误差与偏振串扰误差。

3.3　±45°法

±45°法是一种将半波片置于接收光路中, 通

过旋转两次半波片(相对于初始位置,分别旋转+22.5°与−22.5°)以完成增益比定标的方法。该方法由德国慕尼黑大学的 Freudenthaler 等人提出[15]。±45°法在+45°法的基础上同时考虑了对准偏失角和偏振串扰的影响。

如图 3(彩图见期刊电子版)所示,将一个半波片放置在 PBS 上游光路中,假设此时激光偏振矢量与 PBS 入射面存在初始对准偏失角θ_{init},θ_{h}为人为定量引入的对准偏失角。

半波片旋转之后,由式(4)可得

$$\delta^{*}(\theta_{\mathrm{init}}+\theta_{\mathrm{h}})=\frac{P_{\mathrm{R}}(\theta_{\mathrm{init}}+\theta_{\mathrm{h}})}{P_{\mathrm{T}}(\theta_{\mathrm{init}}+\theta_{\mathrm{h}})}=\frac{[1+\delta\tan^{2}(\theta_{\mathrm{init}}+\theta_{\mathrm{h}})]R_{\mathrm{P}}+[\tan^{2}(\theta_{\mathrm{init}}+\theta_{\mathrm{h}})+\delta]R_{\mathrm{S}}}{[1+\delta\tan^{2}(\theta_{\mathrm{init}}+\theta_{\mathrm{h}})]T_{\mathrm{P}}+[\tan^{2}(\theta_{\mathrm{init}}+\theta_{\mathrm{h}})+\delta]T_{\mathrm{S}}}\cdot G. \tag{9}$$

为了减小初始对准偏失角θ_{init}的影响,±45°法采用连续两次旋转半波片的方式,第一次使半波片相对于初始位置绕光轴顺时针旋转+22.5°,第二次在第一次旋转的基础上使半波片绕光轴逆时针旋转−45°,即相对于初始位置绕光轴逆时针旋转−22.5°,分别使得激光偏振矢量与 PBS 入射面成+45°与−45°,此时增益比G可表示为

$$G=\frac{T_{\mathrm{P}}+T_{\mathrm{S}}}{R_{\mathrm{P}}+R_{\mathrm{S}}}\cdot\sqrt{\delta^{*}(\theta_{\mathrm{init}}+45)\delta^{*}(\theta_{\mathrm{init}}-45)}\quad . \tag{10}$$

由式(10)可以看出,±45°法虽然考虑了 PBS 偏振串扰误差,但无法完全消除对准角误差的影响。事实证明,±45°法的误差来源与信噪比关系不大[16],当θ_{init} = 1°时,G的相对误差可以控制在 5% 以内[15]。由于±45°法操作较为简便且精度较高,目前已经被 MULIS(Multichannel Lidar System)、POLIS(Portable Lidar System)等高精度偏振激光雷达系统用于增益比的定标[16]。其缺点为无法消除对准角误差。

3.4 Δ45°法

Δ45°法是一种将半波片置于接收光路中,通过单方向(顺/逆时针均可)旋转 45°半波片以完成增益比定标的方法(其与+45°法的操作方法一样,但计算方式不同,且无需进行初始 0°角搜寻)。该方法由浙江大学罗敬等人提出[17]。

如图 4 所示,将一个半波片置于 PBS 的上游光路中,假设此时激光偏振矢量与 PBS 入射面存在初始对准偏失角。

半波片旋转之前由式(4)可得

$$\begin{cases}P_{\mathrm{R}}(\theta_{\mathrm{init}})=\left\{\left[P_{S'}\sin^{2}(\theta_{\mathrm{init}})+P_{P'}\cos^{2}(\theta_{\mathrm{init}})\right]R_{\mathrm{P}}+\left[P_{S'}\cos^{2}(\theta_{\mathrm{init}})+P_{P'}\sin^{2}(\theta_{\mathrm{init}})\right]R_{\mathrm{S}}\right\}K_{\mathrm{R}}\\ P_{\mathrm{T}}(\theta_{\mathrm{init}})=\left\{\left[P_{S'}\sin^{2}(\theta_{\mathrm{init}})+P_{P'}\cos^{2}(\theta_{\mathrm{init}})\right]T_{\mathrm{P}}+\left[P_{S'}\cos^{2}(\theta_{\mathrm{init}})+P_{P'}\sin^{2}(\theta_{\mathrm{init}})\right]T_{\mathrm{S}}\right\}K_{\mathrm{T}}\end{cases}. \tag{11}$$

然后将半波片绕光轴旋转,如图 4(b) 所示,旋转之后式(11)中的$P_{\mathrm{R}}(\theta_{\mathrm{init}})$与$P_{\mathrm{T}}(\theta_{\mathrm{init}})$变为$P'_{\mathrm{R}}(\theta_{\mathrm{init}}+90°)$与$P'_{\mathrm{T}}(\theta_{\mathrm{init}}+90°)$,具体公式不再赘述,此时增益比可表示为

$$G=\frac{P_{\mathrm{R}}(\theta_{\mathrm{init}})+P'_{\mathrm{R}}(\theta_{\mathrm{init}}+90°)}{P_{\mathrm{T}}(\theta_{\mathrm{init}})+P'_{\mathrm{T}}(\theta_{\mathrm{init}}+90°)}\cdot\frac{T_{\mathrm{P}}+T_{\mathrm{S}}}{R_{\mathrm{P}}+R_{\mathrm{S}}}\quad , \tag{12}$$

式中,$P_{\mathrm{T}}(\theta_{\mathrm{init}})$、$P_{\mathrm{R}}(\theta_{\mathrm{init}})$、$P'_{\mathrm{T}}(\theta_{\mathrm{init}}+90°)$与$P'_{\mathrm{R}}(\theta_{\mathrm{init}}+90°)$可认为是已知量。通过式(12)可以明显看出,Δ45°法不仅消除了对准角误差,而且同时也减少了偏振串扰误差。不仅如此,激光偏振矢量初始朝向可以是任意角度,这避免了旋转半波片前调整半波片快轴朝向的步骤。Δ45°法在提升定标速度的同时还保证了定标精度,然而其缺点无法排除大气状态变化的影响。

3.5 旋转拟合法

旋转拟合法是一种将半波片置于接收光路中,通过多次旋转半波片,采用非线性最小二乘法拟合同时反演增益比、退偏比以及初始对准偏失角θ_{init}以完成增益比定标的方法。该方法由美国宇航局的 ALVAREZ 等人提出[18]。

如图 5 所示,将一个半波片放置于 PBS 上游的光路中,假设此时激光偏振矢量与 PBS 入射面存在初始对准偏失角θ_{init}。

如果人为控制半波片相对于其初始光轴位置旋转$\theta_{\mathrm{h},j}/2$角,可获得一系列由人为定量引入的对准偏失角$\theta_{\mathrm{h},j}$。则由式(9)可得

$$\delta^{*}(\theta_{\mathrm{init}}+\theta_{\mathrm{h},j})=\frac{P_{\mathrm{R}}(\theta_{\mathrm{init}}+\theta_{\mathrm{h},j})}{P_{\mathrm{T}}(\theta_{\mathrm{init}}+\theta_{\mathrm{h},j})}=\frac{[1+\delta\tan^{2}(\theta_{\mathrm{init}}+\theta_{\mathrm{h},j})]R_{\mathrm{P}}+[\tan^{2}(\theta_{\mathrm{init}}+\theta_{\mathrm{h},j})+\delta]R_{\mathrm{S}}}{[1+\delta\tan^{2}(\theta_{\mathrm{init}}+\theta_{\mathrm{h},j})]T_{\mathrm{P}}+[\tan^{2}(\theta_{\mathrm{init}}+\theta_{\mathrm{h},j})+\delta]T_{\mathrm{S}}}\cdot G, \tag{13}$$

式中,j代表第j次旋转半波片。观察式(13),由于$\delta^{*}(\theta_{\mathrm{init}}+\theta_{\mathrm{h},j})$、$\theta_{\mathrm{h},j}$、$R_{\mathrm{P}}$、$R_{\mathrm{S}}$、$T_{\mathrm{P}}$与$T_{\mathrm{S}}$可认为是已知量,那么式(13)中只有 3 个未知量,即增益比G、初始对准偏失角θ_{init}以及理论退偏比δ。此时一个方程

无法求解 3 个未知数，但由于多次旋转半波片可得到多个方程，采用非线性最小二乘法对该方程组进行求解，即可解出 3 个未知数。需要注意的是，该方法要求至少得到 3 个方程，即$j \geqslant 3$。

该方法的优点为一次定标可同时反演增益比、退偏比以及初始对准偏失角 3 个未知量，并且不需要知道先验值。其缺点为定标耗时较长，操作繁琐，只适用于相对稳定的大气环境下。

3.6　退偏器法

退偏器法是一种通过在光路中添加光学元件将系统接收的回波信号转换为非偏振光以完成增益比定标的方法。其利用两路探测通道信号强度之比进行定标，由式(4)可求解增益比G

$$G=\frac{P_{\mathrm{R}}}{P_{\mathrm{T}}} \quad . \tag{14}$$

其中较为典型的是 CALIOP 利用退偏器产生的非退偏光信号来进行增益比定标[19]。具体操作为在 PBS 上游光路放置一个可移动的退偏器，系统定标时将其置于光路中，定标结束后移出光路，如图 6 所示。CALIOP 采用该方法在夜间轨道上对系统进行增益比定标，并采用洁净大气分子法进行验证[20]。

该方法优点为操作简便并且可进行实时定标，从而排除大气状态改变造成的影响。其缺点为商用退偏器还难以产生完全的退偏光，易引入其它误差。

4　实验结果与分析

实验所采用偏振激光雷达为典型的双通道激光雷达，系统结构如图 1 所示(图中相同的器件只标注一次)。其中介于会聚透镜与半波片之间的退偏器只有在采用退偏器法定标时才会使用，其它时候不需要使用该光学器件。为了减少线偏振度误差，实验系统在出射光路中添加了起偏棱镜，使得出射激光的消光比达到了2×10^5 ∶ 1。为了减少偏振串扰误差，实验系统采用 PBS 与偏振片胶合的结构，使得$T_{\mathrm{P}}:T_{\mathrm{S}}(R_{\mathrm{S}}:R_{\mathrm{P}})>30\,000$ ∶ 1。因此，本文暂不讨论线偏振度误差与偏振串扰误差，只讨论对准误差对增益比造成的影响。系统的具体参数如表 1 所示

由于洁净大气分子法定标误差较大，因此，本文实验主要对比分析了采用+45°法、±45°法、Δ45°法、旋转拟合法与退偏器法等 5 种方法在不同对准偏失角(对准角误差)情况下对增益比定标的影响。

为保证实验有较高的信噪比，实验时间选在夜间。同时，为了减少大气变化而带来影响，选取水平方向(俯仰角为 0°)探测。在完成系统光轴校准后，使用电动旋转电机(精度为 0.005°)调整半波片到激光偏振矢量与 PBS 入射面平行的位置(目测透射通道平均信号最大时即为对应位置)，此时半波片的角度为 0°初始值。需要注意的是，为了表述方便，下文在人为定量引入对准偏失角θ_{h}时，未将初始对准偏失角θ_{init}表示在实际总的对准偏失角中，但实际上每个对准偏失角都包含了初始对准偏失角θ_{init}(θ_{init}属于未知量)。然后，以θ_{h}=0°(实际对准偏失角为θ_{init}+0°)作为零点，使用电动旋转电机旋转半波片。一般来说，在实际操作过程中对准偏失角不会超过 15°[21-22]，但为了实验的完整性，本文将对准偏失角的讨论扩大至 45°。

+45°法、±45°法、Δ45°法与旋转拟合法均以 2.5°为间隔旋转半波片得到θ_{h}=−45°~67.5°情况下共 46 组原始回波信号。通过对上述数据进行处理，+45°法、±45°法、Δ45°法与旋转拟合法 4 种方法均选择 5°为间隔，选取θ_{h}的范围为−45° ~ +45°，(即每组数据两个角度在半波片旋转前后相差 45°)，计算后一共可获得 19 组增益比数据。

采用退偏器法时，在开始实验之前需要在系统光路中添加退偏器，如图 1 所示。由于退偏器是非理想的，为了观察其至少一个周期的变化，退偏器法以 10°为间隔转半波片得到θ_{h}从 −80°到+100°情况下共 19 组原始回波信号，通过对上述数据进行处理，一共可获得 19 组增益比数据。

表 2 是当θ_{h}=0°时，5 种方法的定标结果。观察表 2 可以发现，当没有对准偏失角时，±45°法、Δ45°法与旋转拟合法定标结果较为接近，可以认为上述 3 种方法在θ_{h}=0°时最接近真实值。令上述 3 种方法在θ_{h}=0°时测得增益比的平均值为真实值，并绘制出如图 7 所示的 5 种定标方法的相对误差随对准偏失角的变化曲线(旋转拟合法与退偏器法计算过程详见 4.2 与 4.3 节)。

4.1 +45°、±45°、Δ45°法

如图 7 所示，当$|\theta_h|$<15°时，±45°法与Δ45°法的定标结果相近，相对误差也较小，而+45°即使不存在对准偏失角时，定标结果也与上述两种方法存在较大差异，相对误差可达 4%。当$|\theta_h|$>15°时，+45°法与Δ45°法的定标结果总体保持稳定，而±45°法的定标结果随对准偏失角的增大而变得不稳定，相对误差急剧增大，甚至高达 12.93%。±45°法出现这样误差分布的原因主要在于其计算前后两次测量数据的几何平均，而Δ45°法则是在+45°法的基础上计算前后两次测量数据的算术平均。下文将通过具体理论分析来解释+45°法出现上述现象的原因。

对两种方法进行相对误差分析[23-24]，令两种方法旋转半波片前后反射通道与透射通道探测到的功率分别为$P_{\mathrm{R}}^{\mathrm{a}}$、$P_{\mathrm{R}}^{\mathrm{b}}$与$P_{\mathrm{T}}^{\mathrm{a}}$、$P_{\mathrm{T}}^{\mathrm{b}}$，可得

$$(\delta_1)^2=\left(\frac{\Delta G_{\Delta 45^\circ}}{G_{\Delta 45^\circ}}\right)^2=\frac{(\Delta P_{\mathrm{R}}^{\mathrm{a}})^2+(\Delta P_{\mathrm{R}}^{\mathrm{b}})^2}{(P_{\mathrm{R}}^{\mathrm{a}}+P_{\mathrm{R}}^{\mathrm{b}})^2}+\frac{(\Delta P_{\mathrm{T}}^{\mathrm{a}})^2+(\Delta P_{\mathrm{T}}^{\mathrm{b}})^2}{(P_{\mathrm{T}}^{\mathrm{a}}+P_{\mathrm{T}}^{\mathrm{b}})^2}\quad,\tag{15}$$

$$(\delta_2)^2=\left(\frac{\Delta G_{+45^\circ}}{G_{+45^\circ}}\right)^2=\frac{1}{4}\left(\frac{\Delta P_{\mathrm{R}}^{\mathrm{a}}}{P_{\mathrm{R}}^{\mathrm{a}}}\right)^2+\frac{1}{4}\left(\frac{\Delta P_{\mathrm{R}}^{\mathrm{b}}}{P_{\mathrm{R}}^{\mathrm{b}}}\right)^2+\frac{1}{4}\left(\frac{\Delta P_{\mathrm{T}}^{\mathrm{a}}}{P_{\mathrm{T}}^{\mathrm{a}}}\right)^2+\frac{1}{4}\left(\frac{\Delta P_{\mathrm{T}}^{\mathrm{b}}}{P_{\mathrm{T}}^{\mathrm{b}}}\right)^2\quad,\tag{16}$$

式中δ_1与δ_2分别代表Δ45°法与±45°法定标结果的相对误差，ΔP_S^n（S为R,T且n为a, b）代表各个测量值的不确定度（标准差）。激光雷达中光子计数的信号可以认为服从泊松分布[25-26]，因此统计误差等于信号平均值的均方根，即$\Delta I=\sqrt{I}$，因此，式(15)与式(16)可进一步推导为

$$(\delta_1)^2=\frac{1}{P_{\mathrm{R}}^{\mathrm{a}}+P_{\mathrm{R}}^{\mathrm{b}}}+\frac{1}{P_{\mathrm{T}}^{\mathrm{a}}+P_{\mathrm{T}}^{\mathrm{b}}}\quad,\tag{17}$$

$$(\delta_2)^2=\frac{1}{4P_{\mathrm{R}}^{\mathrm{a}}}+\frac{1}{4P_{\mathrm{R}}^{\mathrm{b}}}+\frac{1}{4P_{\mathrm{T}}^{\mathrm{a}}}+\frac{1}{4P_{\mathrm{T}}^{\mathrm{b}}}\quad.\tag{18}$$

$(\delta_1)^2$与$(\delta_2)^2$作差可发现，$(\delta_1)^2\leqslant(\delta_2)^2$，即Δ45°法的不确定度小于等于±45°法。事实上，根据实验结果，±45°法在对准偏失角较大的情况下，定标的增益比廓线的振荡幅度的确要大于Δ45°法，这也解释了图 7 中±45°法在对准偏失角较大的情况下，误差远大于Δ45°法的原因。

4.2 旋转拟合法

考虑到实际过程中对准偏失角的误差不会超过 15°，选择$|\theta_h|\leqslant$15°的 13 组数据（即$\theta_{h,j}$=0°, ±2.5°, ±5°…±15°）进行数据拟合，旋转拟合法计算结果如图 8（彩图见期刊电子版）所示，其中蓝色圆圈代表在不同θ_{h}情况下的$\delta^*(\theta)$，由式可知，求解增益比 G、初始对准偏失角θ_{init}以及理论退偏比δ 3 个未知数的方程组属于非线性最小二乘法问题。求解之前需要对 G、θ_{init}与δ 3 个未知数的初始值进行预测。为了得到最佳初始预测值，由图 8 可知，$\delta^*(\theta_{\mathrm{init}}+\theta_{\mathrm{h},j})$与$\theta_{\mathrm{h},j}$之间的关系（蓝色圆圈）可以近似用一个二次多项式来表示[27]，故以人为定量引入对准偏失角$\theta_{\mathrm{h},j}$为自变量，实际测量退偏比$\delta^*(\theta_{\mathrm{init}}+\theta_{\mathrm{h},j})$为应变量构建如下二次多项式

$$\delta^*(\theta_{\mathrm{init}}+\theta_{\mathrm{h},j})^*=A_0+A_1\times\theta_{\mathrm{h},j}+A_2\times\theta_{\mathrm{h},j}{}^2\quad,\tag{19}$$

式中，A_0、A_1与A_2均为二次多项式系数。拟合结果如图 8 中红色虚线所示，该二次多项式的最小值即代表初始对准偏失角θ_{init}，计算结果$\theta_{\mathrm{init}}=-A_1/(2\times A_2)=-0.35°$，该值可作为$\theta_{\mathrm{init}}$的最佳初始预测值。接着，将$\theta_{\mathrm{init}}=-0.35°$代入式(13)并使用非线性最小二乘法求解方程组，求得增益比G=1.271 6。

4.3 退偏器法

退偏器法计算结果如图 9（彩图见期刊电子版）所示，其中蓝色圆圈代表在半波片不同角度下计算的增益比，观察各蓝色圆圈的分布情况，可知其较为符合余弦曲线分布规律。故以半波片旋转角度φ ($\theta_{\mathrm{h}}=2\varphi$) 为自变量，增益比$G$为应变量构建如下余弦函数多项式

$$G=B_0\cos(B_1\times\varphi+B_2)+B_3\quad,\tag{20}$$

式中，B_0、B_1、B_2与B_3均代表余弦函数多项式的系数。拟合的结果如图 9 中红色虚线所示

从理论上来说，假如回波信号为完全的非偏振光，那么无论如何改变半波片的角度都无法改变非偏振光的状态。换句话说，旋转半波片并不会影响增益比的数值，增益比定标的结果应该表征为一条平行于 x 轴的直线，而非像图 9 中那样表现为余弦的分布情况。导致该问题的原因是目前商用退偏器无法将偏振光完全转化为非偏振光，回波信号在经过退偏器之后仍包含一部分的

偏振光。浙江大学罗敬等人以激光为光源，在测试退偏器的退偏效果时，发现测试结果也类似图 9 中余弦分布的情况[28]。这说明即使在对准偏失角为0°的情况下，增益比定标结果仍会受到该部分偏振光的影响。

需要注意的是，退偏器法测量的数据中只有 5 组数据的对准偏失角在−45° ~ +45°内，所以该种方法在图 7 中只标有 5 个点。退偏器法在 θ_h=0°时，相对误差为 5.6%。这说明即使在对准偏失角为 0°的情况下，增益比定标结果仍会受到该部分偏振光的影响。

4.4　讨论

通过对实验结果进行分析，可得知±45°法、Δ45°法与旋转拟合法定标结果最为准确，这和前文的理论分析一致。但是±45°法在对准偏失角较大的情况下误差较大。旋转拟合法定标耗时较长，操作繁琐，只适用于相对稳定的大气环境下。相比之下，Δ45°法操作更为简便，定标结果不受对准偏失角的影响，而且也无需进行初始 0°角的搜寻，优势明显。但是，Δ45°法也无法排除大气状态变化的影响，相比之下，只有退偏器法同时具有操作简便，可排除大气状态变化影响的能力，而且也不存在多次旋转半波片会增加角度积累误差的问题，但目前商用退偏器仍无法产生完全的退偏光，这会引入新的误差，且难以评估。综上所述，建议偏振激光雷达研究人员在一般情况下采用Δ45°法定标，在有高精度退偏器的情况下采用退偏器法定标。

5　结　论

增益比的定标准确性对偏振激光雷达探测精度影响很大。本文系首次在原理与实验上对比了现存多种增益比定标方法，并给相关研究人员提出了增益比定标方法选择的指导意见。

就可操作性而言，退偏器法只需在系统中插入退偏器即可完成定标，可排除大气状态改变造成的影响，而其余需要旋转半波片的 4 种方法至少需要完成两次旋转，操作相对复杂，而且无法排除大气状态改变造成的影响。就定标准确性而言，实验主要对比了+45°法、±45°法、Δ45°法、旋转拟合法与退偏器法等 5 种方法（由于洁净大气分子法定标误差较大，本文未作实验对比）在不同对准偏失角下对增益比定标的影响。实验结果表明，±45°法、Δ45°法与旋转拟合法的定标准确度相对较高，但±45°法与旋转拟合法操作较为复杂。±45°法在对准偏失角较大的情况下误差较大。Δ45°法增益比定标结果不受对准偏失角的影响，而且也无需进行初始 0°角的搜寻。+45°法相对于前 3 种方法在没有对准偏失角的情况下误差更大。退偏器法受到非理想退偏器的影响较大，如果存在理想退偏器，那么这种方法将是一种理想的增益比定标方法。通过对不同增益比定标方法理论与实验的对比，本文给出了增益比定标方法的最佳选择，即建议在一般情况下采用Δ45°法定标，有高精度退偏器的情况下采用退偏器法定标。

References:

[1] SCHOTLAND R M, SASSEN K, STONE R. Observations by lidar of linear depolarization ratios for hydrometeors[J]. *Journal of Applied Meteorology*, 1971, 10(5): 1011-1017.

[2] SASSEN K. Polarization in lidar: a review[J]. *Proceedings of SPIE*, 2003, 5158: 151-160.

[3] LIU D, YANG Y Y, ZHANG Y P, *et al*.. Pattern recognition model for aerosol classification with atmospheric backscatter lidars: principles and simulations[J]. *Journal of Applied Remote Sensing*, 2015, 9(1): 096006.

[4] 成中涛, 刘东, 罗敬, 等. 视场展宽迈克耳孙光谱滤光器增透膜容差评估[J]. 中国激光, 2015, 42(8): 0813002.
CHENG ZH T, LIU D, LUO J, *et al*.. Tolerance evaluation for anti-reflection coatings in field-widened michelson spectroscopic filter[J]. *Chinese Journal of Lasers*, 2015, 42(8): 0813002. (in Chinese)

[5] QIU J W, XIA H Y, SHANGGUAN M J, *et al*.. Micro-pulse polarization lidar at 1.5 μm using a single superconducting nanowire single-photon detector[J]. *Optics Letters*, 2017, 42(21): 4454-4457.

[6] GOBBI G P, BARNABA F, GIORGI R, *et al*.. Altitude-resolved properties of a Saharan dust event over the Mediterranean[J]. *Atmospheric Environment*, 2000, 34(29-30): 5119-5127.

[7] DIONISI D, BARNABA F, COSTABILE F, *et al*.. Retrieval of aerosol parameters from continuous h24 lidar-ceilometer measurements[J]. *EPJ Web of Conferences*, 2016, 119(4): 23004.

[8] BINIETOGLOU I, AMODEO A, D'AMICO G, *et al*.. Examination of possible synergy between lidar and ceilometer for the monitoring of atmospheric aerosols[J]. *Proceedings of SPIE*, 2011, 8182: 818209.

[9] CAIRO F, DI DONFRANCESCO G, ADRIANI A, *et al*.. Comparison of various linear depolarization parameters measured by lidar[J]. *Applied Optics*, 1999, 38(21): 4425-4432.

[10] 罗敬, 刘东, 徐沛拓, 等. 基于偏振分光棱镜的高精度偏振分光系统[J]. 中国激光, 2016, 43(12): 1210001.
LUO J, LIU D, XU P T, *et al*.. High-precision polarizing beam splitting system based on polarizing beam splitter[J]. *Chinese Journal of Lasers*, 2016, 43(12): 1210001. (in Chinese)

[11] BEHRENDT A, NAKAMURA T. Calculation of the calibration constant of polarization lidar and its dependency on atmospheric temperature[J]. *Optics Express*, 2002, 10(16): 805-817.

[12] YOUNG A T. Rayleigh scattering[J]. *Physics Today*, 1982, 35(1): 42-48.

[13] SHE C Y. Spectral structure of laser light scattering revisited: bandwidths of nonresonant scattering lidars[J]. *Applied Optics*, 2001, 40(27): 4875-4884.

[14] LUO J, LIU D, HUANG Z H, *et al*.. Polarization properties of receiving telescopes in atmospheric remote sensing polarization lidars[J]. *Applied Optics*, 2017, 56(24): 6837-6845.

[15] FREUDENTHALER V, ESSELBORN M, WIEGNER M, *et al*.. Depolarization ratio profiling at several wavelengths in pure Saharan dust during SAMUM 2006[J]. *Tellus B*: *Chemical and Physical Meteorology*, 2009, 61(1): 165-179.

[16] SASSEN K, BENSON S. A midlatitude cirrus cloud climatology from the facility for atmospheric remote sensing. Part II: microphysical properties derived from lidar depolarization[J]. *Journal of the Atmospheric Sciences*, 2001, 58(15): 2103-2112.

[17] LUO J, LIU D, BI L, *et al*.. Rotating a half-wave plate by 45°: an ideal calibration method for the gain ratio in polarization lidars[J]. *Optics Communications*, 2018, 407: 361-366.

[18] ALVAREZ J M, VAUGHAN M A, HOSTETLER C A, *et al*.. Calibration technique for polarization-sensitive lidars[J]. *Journal of Atmospheric and Oceanic Technology*, 2006, 23(5): 683-699.

[19] MATTIS I, TESCHE M, GREIN M, *et al*.. Systematic error of lidar profiles caused by a polarization-dependent receiver transmission: quantification and error correction scheme[J]. *Applied Optics*, 2009, 48(14): 2742-2751.

[20] HUNT W H, WINKER D M, VAUGHAN M A, *et al*.. *CALIPSO* lidar description and performance assessment[J]. *Journal of Atmospheric and Oceanic Technology*, 2008, 26(7): 1214-1228.

[21] 曲艺. 大气光学遥感监测技术现状与发展趋势[J]. 中国光学, 2013, 6(6): 834-840.
QU Y. Technical status and development tendency of atmosphere optical remote and monitoring[J]. *Chinese Optics*, 2013, 6(6): 834-840. (in Chinese)

[22] 杨子健, 陈锋, 李抄, 等. 微脉冲激光雷达中的光子计数死区时间瞬态效应[J]. 光学 精密工程, 2015, 23(2): 408-414.
YANG Z J, CHEN F, LI CH, *et al*.. Transient effect of dead time of photon-counting in micro-pulse lidar[J]. *Optics and Precision Engineering*, 2015, 23(2): 408-414. (in Chinese)

[23] 段绿林, 刘东, 张与鹏, 等. 基于混合智能算法的激光雷达数据拼接技术[J]. 光学学报, 2017, 37(6): 0601002.
DUAN L L, LIU D, ZHANG Y P, *et al*.. Lidar data gluing technology based on hybrid intelligent algorithm[J]. *Acta Optica Sinica*, 2017, 37(6): 0601002. (in Chinese)

[24] LUO J, LIU D, WANG B Y, *et al*.. Effects of a nonideal half-wave plate on the gain ratio calibration measurements in polarization lidars[J]. *Applied Optics*, 2017, 56(29): 8100-8108.

[25] D'AMICO G, AMODEO A, MATTIS I, *et al*.. EARLINET single calculus chain - technical - Part 1: pre-processing of raw lidar data[J]. *Atmospheric Measurement Techniques*, 2016, 9(2): 491-507.

[26] 刘群, 刘崇, 朱小磊, 等. 星载海洋激光雷达最佳工作波长分析[J]. 中国光学, 2020, 13(1): 148-155.
LIU Q, LIU CH, ZHU X L, *et al*.. Analysis of the optimal operating wavelength of spaceborne oceanic lidar[J]. *Chinese Optics*, 2020, 13(1): 148-155. (in Chinese)

[27] 鲁先洋, 李学彬, 秦武斌, 等. 微脉冲激光雷达反演气溶胶的水平分布[J]. 光学 精密工程, 2017, 25(7): 1697-1704.
LU X Y, LI X B, QIN W B, *et al*.. Retrieval of horizontal distribution of aerosol mass concentration by micro pulse lidar[J]. *Optics and Precision Engineering*, 2017, 25(7): 1697-1704. (in Chinese)

[28] 成中涛, 刘东, 罗敬, 等. 光谱滤光器透射率参数对高光谱分辨率激光雷达的影响分析[J]. 光学学报, 2014, 34(8): 0801003.

CHENG ZH T, LIU D, LUO J, *et al*.. Influences analysis of the spectral filter transmission on the performance of high-spectral-resolution lidar[J]. *Acta Optica Sinica*, 2014, 34(8): 0801003. (in Chinese)

Author Biographics:

Tong Yicheng (1994—), male, born in Ningbo City, Zhejiang Province. He is a doctoral candidate. In 2018, he obtained his bachelor's degree from Changchun University of Science and Technology. He is mainly engaged in the research of atmospheric remote sensing lidar. E-mail: yichengtong@zju.edu.cn

童奕澄(1994—), 男, 浙江宁波人, 博士研究生, 2018 年于长春理工大学获得学士学位, 主要从事大气遥感激光雷达方面的研究。E-mail: yichengtong@zju.edu.cn

Liu Dong (1982—), male, born in Dalian City, Liaoning Province. He is a doctor, professor and doctoral supervisor. He obtained his bachelor's degree and doctor's degree from Zhejiang University in 2005 and 2010 respectively. He is mainly engaged in the research of photoelectric detection and lidar. E-mail: liudongopt@zju.edu.cn

刘　东(1982—), 男, 辽宁大连人, 博士, 教授, 博士生导师, 2005 年、2010 年于浙江大学分别获得学士、博士学位, 主要从事光电检测与激光雷达等方面的研究。E-mail: liudongopt@zju.edu.cn